PERIOD-DOUBLING BIFURCATIONS OF THE ATMOSPHERIC CIRCULATION AND APERIODIC VARIATIONS OF THE FLOW PATTERNS

Luo Zhexian (罗哲贤)

Gansu Research Institute of Meteorological Science, Lanzhou

Received November 17, 1986

ABSTRACT

An eighth-order set of ordinary differential equations, which governs the dynamics of a quasi-geostrophic flow of the baroclinic atmosphere, is used to investigate bifurcational and chaotic forms of the atmospheric circulation. Numerical integrations of the set exhibit period-doubling bifurcations of the flow patterns. It would seem that the Feigenbaum relation $(r_n-r_{n-1})/(r_{n+1}-r_n)=4.6692$ is satisfied approximately. Above a limit point the solutions are aperiodic and chaotic, and a strange attractor having four inter-linked chaotic fragments appears. A window of period-6 emerges also in the chaotic region.

I. INTRODUCTION

Using a three-variable, deterministic, and nonlinear autonomous system, Lorenz (1963) first found that the numerically determined solutions of the system (hereinafter are called strange attractors) are generally aperiodic and chaotic in certain parametric combination. Since the 1970s, a lot of work concerning the Lorenz's system has been done. Meantime, Feigenbaum (1978) put forward the concept about universality of period-doubling bifurcations of nonlinear systems. Because the Lorenz's system was derived from the small scale convection equations provided by Saltzman (1961), it must be solved how to translate from periodic to chaotic states for the forced and dissipative systems describing the evolution of flow pattern of large-scale atmospheric motions. In this paper we introduce an eighth-order set of nonlinear equations governing the dynamics of quasi-geostrophic current, and it can exhibit intermittent chaos through the way of period-doubling bifurcations.

II. MODEL

The subscripts 1,2, and 3 are used to denote the levels of 250, 500, and 750 hPa, respectively. Thus the geostrophic vorticity equation at levels 1 and 3, and the thermodynamic equation at level 2 can be respectively written as

$$\frac{\partial}{\partial t}\nabla^2\psi_1+J(\psi_1,\nabla^2\psi_1+\beta^*y)=f_0\cdot\frac{\omega_2}{\Delta p}-k_d'\nabla^2(\psi_1-\psi_3), \tag{1}$$

$$\frac{\partial}{\partial t}\nabla^2\psi_3+J(\psi_3,\nabla^2\psi_3+\beta^*y)=-f_0\frac{\omega_2}{\Delta p}+k_d'\nabla^2(\psi_1-\psi_3)-k_d\nabla^2\psi_3, \tag{2}$$

$$\frac{\partial}{\partial t}(\psi_1-\psi_3)+J(\psi_2,\psi_1-\psi_3)=\lambda^2\frac{f_0}{\Delta p}\omega_2+\lambda^2 h_d'[(\psi_1-\psi_3)^*-(\psi_1-\psi_3)], \tag{3}$$

where ψ_i is the geostrophic streamfunction at level i, ω_2 the individual pressure change, $\beta^*=df/dy$, f is the Coriolis parameter, k_d, k_d' are quantities representing vortex stretching due to frictional convergence in the boundary layer and vertical internal friction, respectively. λ is the Rossby radius of deformation, $(\lambda^2 h_d')^{-1}$ the thermal relaxation time, and $(\psi_1-\psi_3)^*$ the given thermal forcing parameter.

Let

$$\begin{aligned}&(x,y,t,\psi_1,\psi_2,\psi_3,\omega_2,\beta^*,\lambda^2,k_d,k_d',h_d')\\&=(Lx',Ly',f_0^{-1}t',L^2f_0\psi_1',L^2f_0\psi_2',L^2f_0\psi_3',f_0\Delta p\omega_2',f_0L^{-1}\beta^{*\prime},\\&2L^2\sigma',2f_0K,f_0K_1',L^{-2}f_0h_1'),\end{aligned} \tag{4}$$

where $\Delta P=P_3-P_1=500$ hPa, L is the horizontal wavelength and taken to be 1.83×10^8 cm.

Substituting (4) into (1)—(3), the nondimensional equation set can be obtained. Let

$$\psi_1\equiv\psi+\theta,\ \psi_3\equiv\psi-\theta,\ \psi_2\equiv\psi,\ (\psi_1-\psi_3)^*=2\theta^*,\ (\psi,\theta,\theta^*)=\sum_{i=A,K,C,N}(\psi_i,\theta_i,\theta_i^*)F_i \tag{5}$$

where $F_A=\sqrt{2}\cos y$, $F_K=2\cos Nx\sin y$, $F_C=\sqrt{2}\cos 2y$, $F_N=2\sin Nx\sin 2y$. N is the zonal wavenumber in the beta-plane. The model atmosphere is confined to a periodic beta-plane channel with zonal walls at $y=0$ and $y=\pi$; at the median line of the beta-plane, $\varphi=\varphi_0=40°$N.

Substituting (5) into the nondimensional forms of Eqs. (1)—(3), we have the spectral system:

$$\dot\psi_A=-K(\psi_A-\theta_A), \tag{6}$$

$$\dot\theta_A=\frac{h''}{1+\sigma}\theta_A^*-\frac{h''+\sigma(2K_1+K)}{1+\sigma}\theta_A+\frac{\sigma K}{1+\sigma}\psi_A, \tag{7}$$

$$\dot\psi_K=-\beta a''(\psi_C\psi_N+\theta_C\theta_N)-K(\psi_K-\theta_K), \tag{8}$$

$$\dot\psi_C=\varepsilon a''(\psi_K\psi_N+\theta_K\theta_N)-K(\psi_C-\theta_C), \tag{9}$$

$$\dot\psi_N=\delta' a''(\psi_K\psi_C+\theta_K\theta_C)-K(\psi_N-\theta_N), \tag{10}$$

$$\begin{aligned}\dot\theta_K=\frac{-1}{1-\beta+\sigma}\{&a''(\sigma\beta+1-\beta)\psi_C\theta_N+a''(\sigma\beta-1+\beta)\psi_N\theta_C\\&-K\sigma\psi_K-(1-\beta)h''\theta_K^*+[\sigma(2K_1+K)+(1-\beta)h'']\theta_K\},\end{aligned} \tag{11}$$

$$\begin{aligned}\dot\theta_C=\frac{1}{1-\varepsilon+\sigma}\{&a''(\sigma\varepsilon-1+\varepsilon)\psi_N\theta_K+a''(\sigma\varepsilon+1-\varepsilon)\psi_K\theta_N+\sigma K\psi_C+\\&+(1-\varepsilon)h''\theta_C^*-[\sigma(2K_1+K)+(1-\varepsilon)h'']\theta_C\},\end{aligned} \tag{12}$$

$$\begin{aligned}\dot\theta_N=\frac{1}{1-\beta'+\sigma}\{&a''(\sigma\delta'-1+\beta')\psi_K\theta_C+a''(\sigma\delta'+1-\beta')\psi_C\theta_K+\\&+\sigma K\psi_N-[\sigma(2K_1+K)+(1-\beta')h'']\theta_N\},\end{aligned} \tag{13}$$

where $\beta=\dfrac{N^2}{N^2+1}$, $a''=\dfrac{64\sqrt{2}N}{15\pi}$, $\varepsilon=\dfrac{3}{4}$, $\delta'=\dfrac{N^2-3}{N^2+4}$, $\beta'=\dfrac{N^2+3}{N^2+4}$, $h''=\sigma' h_1'$.

Eqs. (6)—(13) form a forced, dissipative, and nonlinear autonomous system containing ψ_i, and θ_i $(i=A,K,C,N)$ as unknown variables. The thermal forcing parameters of the system are θ_A^*, θ_K^* and θ_C^*. $\theta_K^*F_K$ reflects the x-direction thermal forcing including the difference between sea and land. $\theta_A^* F_A$ and $\theta_C^* F_C$ represent the non-uniform heating of wavenumber one and two in south-north direction, respectively. When $\theta_C^* < 0$, it can be relatively cold at low latitudes and heated at middle latitudes. By superposing $\theta_C^* F_C (\theta_C^* < 0)$ on $\theta_A^* F_A (\theta_A^* > 0)$, the heating distribution will be similar to the character of both the solar radiation field and the heating field in summer. The following parametric values are prescribed: $K=0.0057$, $h''=K_1=0.0114$, $\sigma=0.2$, and $\theta_A^*=0.10$, which are the same as those in the paper by Charney and Straus (1980). Substituting these parametric values into Eqs. (6) and (7), gives $\bar{\psi}_A=\bar{\theta}_A=$ 0.07143 and $\bar{u}_1=22.1$ m s^{-1}, where $\bar{\psi}_A$ and $\bar{\theta}_A$ represent the equilibrium solutions of ψ_A and θ_A, and $\bar{u}_1$ is the component of zonally-averaged wind velocity of wavenumber one in the south-north direction at 250 hPa, 22.1 m s^{-1} is a reasonable magnitude in summer. In the case that $\theta_A^*=0.10$, one hundred and twenty values in the range of $-0.12 \leqslant \theta_C^* \leqslant 0$ were impartially selected in order to compute the fields of θ^* by formula (5). The computational results show that when $-0.06 \leqslant \theta_C^* \leqslant -0.039$, the most heated latitudes range from 30 to 33°N. It has well been known that in East Asia the heating centre in the south-north direction in summer is near 30°N rather than near the equator. Therefore, we are going to investigate how the characteristics of evolution of large-scale flow pattern change as θ_C^* varies gradually within the parametric limits of $-0.06 \leqslant \theta_C^* \leqslant -0.039$.

It is easily found that the generalized divergence of Eqs. (6)—(13)

$$D=\sum_{i=A,K,C,N} \frac{\partial \dot{\psi}}{\partial \psi_i}+\frac{\partial \dot{\theta}}{\partial \theta_i}$$

is always smaller than zero, which results in the continuous decrease of the phase volume and the global stability in the process of evolution. On the other hand, the system of Eqs. (6)—(13) contains twelve nonlinear terms which may stimulate the local unstability. The common existence of the global stability and the local unstability is a necessary condition to form the strange attractor.

The numerical integration scheme used here is from Asselin (1972). The time step is taken to be 3 h, and all integrations of Eqs. (6)—(13) are carried out for the period of more than 20000 steps. In certain parametric combinations of the thermal forcings, the period-doubling bifurcations of quasi-geostrophic current may obviously be exhibited.

III. PERIOD-DOUBLING BIFURCATIONS OF LARGE-SCALE ATMOSPHERIC MOTION

The system of Eqs. (6)—(13) consists of two subsystems. The first one defined by Eqs. (6)—(7) can be solved analytically. The second one, a sixth-order set of ordinary nonlinear equations, may be investigated only numerically.

In order to schematically show the integrational results of Eqs. (8)—(13) we let $X \equiv \psi_K + \theta_K$, $Y \equiv \psi_N + \theta_N$, and $Z = \psi_C + \theta_C$, representing the components of geostrophic streamfunction at 250 hPa in K, N, and C directions, respectively. To study the basic characteristics of evolutions of X, Y, Z with time, the suface of section plots is used. When the system orbit in X, Y, and Z space crosses the plane $Z=-0.020$ with $\dot{Z}<0$, we plot its coordinates in the X-Y plane.

Let initial values $\varphi_0=(\psi_{K_0}, \psi_{C_0}, \psi_{N_0}, \theta_{K_0}, \theta_{C_0}, \theta_{N_0})=(-0.01150, -0.04000, -0.00580, -0.00158, -0.04000, -0.00290)$, and $\theta_K^*=0.04$. The closed centers of subtropical highs with a reasonable magnitude appear on the geopotential height field at 250 hPa corresponding to φ_0.

The results of integrations of Eqs. (8)—(13) are as follows;

For $-0.039 \geqslant \theta_c^* > -0.05285$, all integrations lead to the orbits which are asymptotic to the simple limit cycle. Correspondingly, there is only a fixed point on the surface of section (Fig. la for $\theta_c^* = -0.0520$). In the range of $-0.0520 \geqslant \theta_c^* > -0.05285$, fifteen values are selected at equal intervals for integrating the system. When $\theta_c^* = -0.05285$, one fixed point has suddenly become unstable and the point in the surface of section converges toward two points at which the system orbit sequentially passes (Fig. 1b.) We regard a point with $\theta_c^* = -0.05285$ as the first bifurcation point r_1 of period-doubling. Similarly, as θ_c^* reaches -0.05323, another bifurcation from a stable two-fixed point to an unstable two-fixed point and a stable four-fixed point periodic cycle have occurred, as illustrated in Fig. 1c. The point with $\theta_c^* = -0.05323$ is considered as the second bifurcation point r_2 of period-doubling. When $\theta_c^* = -0.053310$, a new bifurcation of period-doubling appears and a stable eight-fixed point periodic cycle has exhibited on the surface of section. The point with $\theta_c^* = -0.053310$ is regarded as the third bifurcation point r_3. Feigenbaum (1978) has thoroughly studied the problem about the inherent relations among bifurcation points of period-doubling for a first-order difference equation and found that

$$\delta_n = (r_n - r_{n-1}) / (r_{n+1} - r_n) \tag{14}$$

is a universal constant being about 4.6692 for large n. Substituting $r_1 = -0.05285$, $r_2 = -0.05323$, and $\delta_2 = 4.6692$ into (14), we can obtain the theoretic value r_3' at which a bifurcation from a stable four-point periodic cycle to a stable eight-point one should be expected theoretically. Comparing the practical value, $r_3 = -0.053310$, with the theoretic value, $r_3' = -0.0533114$, we may judge that they are very close to each other. Similarly, we have also computed the theoretic values $r_4' = -0.0533288$, and $r_5' = -0.05333256$. The former corresponds to the bifurcation point from a stable eight-point periodic motion to a stable sixteen-point one, and the latter from sixteen to thirty two. When $\theta_c^* = -0.053315$ and -0.0533275, which have

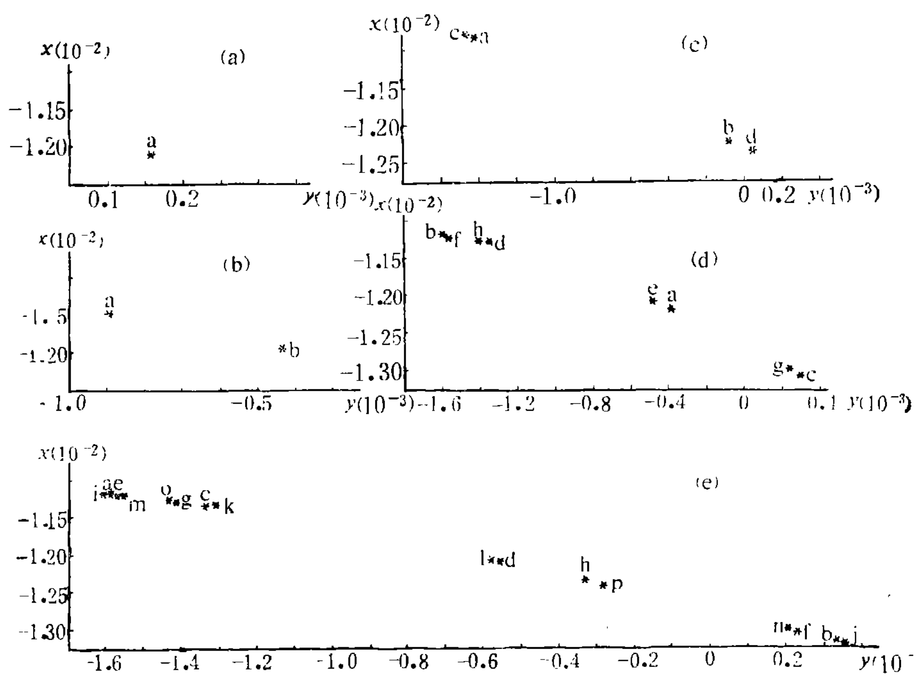

Fig. 1. Period-doubling bifurcations for θ_c^* values of (a) -0.05200, (b) -0.05285, (c) -0.05323, (d) -0.053315, and (e) -0.053330.

not passed through the point r'_4, there are the stable eight-fixed points on the surface of section (see Fig. 1d), but when $\theta_C^*=-0.053330$, which has passed through the point r'_4, the stable sixteen-fixed points on the surface of section appear clearly (Fig. 1e). As $\theta_C^*=-0.053333$, which has got over the point r'_5, the results of the experiment with integration time larger than 130000 time steps show that the stable periodic trajectory with the thirty-two fixed points exists definitely (figure omitted).

To summarize, along with the gradual variation of the thermal forcing parameter θ_C^* within the range of $-0.039 \geqslant \theta_C^* > -0.060$, we have observed a succession of bifurcations from the simple limit cycle, represented by the one-fixed point in the surface of section, to more complicated limit cycles, characterized by the fixed points of periodicity 2^n after n bifurcations, and we have been able to distinguish n as large as 5 by way of numerical integrations of the system of Eqs. (8)—(13), which describes the dynamics of quasi-geostrophic current. And the relation among the bifurcation points is restricted by the Feigenbaum's universal formula.

It can be obtained from (14) (see Pedlosky, 1980) that

$$r_\infty \approx r_1 + \frac{r_2 - r_1}{1-\varepsilon}, \tag{15}$$

where $\varepsilon_1 = 1/4.6692$.

Substituting $r_1=-0.05285$, and $r_2=-0.05323$ into (15), we have got that $r_\infty=-0.0533336$. After θ_C^* passes through the point r_∞, the evolution of flow patterns will exhibit chaotic characteristics rather than multi-periodic states.

IV. APERIODIC EVOLUTION OF LARGE-SCALE ATMOSPHERIC MOTION

Let $\theta_C^*=-0.05334$, which has got over the critical point r_∞, the system of Eqs. (8)—(13) is integrated for 75000 time steps. The points in the surface of section corresponding to this integration approach an aperiodic state, and the system orbit is very strongly attracted to the four segments A, B, C, D (Fig. 2). Compared the aspects in Fig. 2 with those in Fig. 1, the most outstanding difference between them is that there are 2^n ($n=0, 1, 2, 3, 4$) fixed points in Fig. 1, but there are no fixed points on the segments in Fig. 2, which reflects the distinct structures of system orbits and the distinct characteristics of evolution of flow patterns. In the phase space (X, Y, Z), the system orbit for $\theta_C^*=-0.05334$ moves in the following way. The orbit first pierces the surface of section at point 1 on segment A with $\dot{Z}<0$, then at points 2, 3, 4, 5 with $\dot{Z}<0$, successively. Although the points always alternate sequentially in certain order, that is, A→B→C→D→A, there is not any point on the segments which reappear exactly. Thus, there is not any simple or multiple periodic state. To further show the aperiodic characteristics of the system orbit, we define the asymptotic transform functions for a series of the points belonging to the four segments, respectively:

$$Y_{K,n+1}=F(Y_{K,n})=T^{(4)}(Y_{K,n}), \tag{16}$$

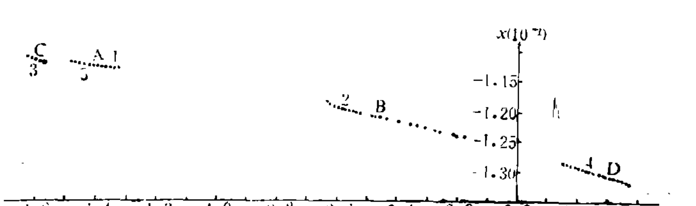

Fig. 2. Surface of section plots for $\theta_C^*=-0.05334$.

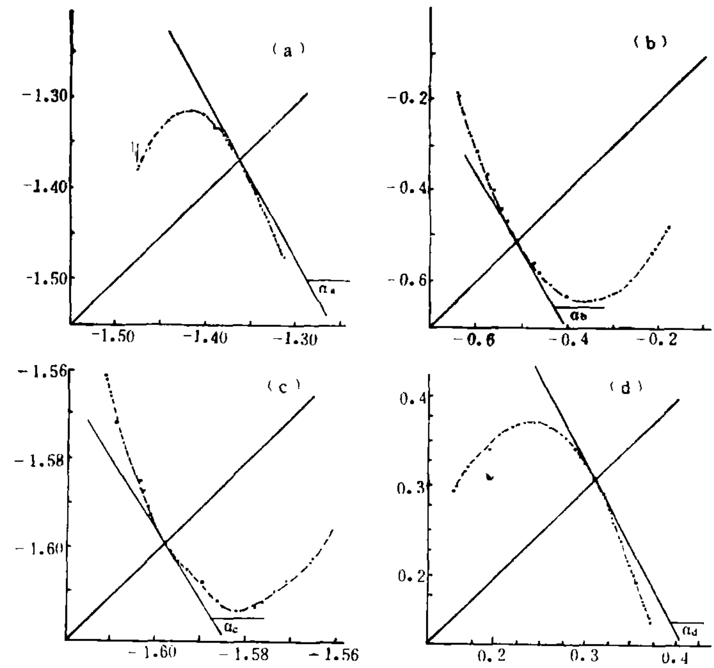

Fig. 3. Asymptotic transform curves corresponding to segments A,B,C,D; the abscissa is $Y_{K,n} \times 10^3$ and the ordinate $Y_{K,n+1} \times 10^3$.

where $K=$ A, B, C, D, $T^{(4)}$ denotes the transform between a given point piercing the surface of section and the last one on the same segment. We have plotted $Y_{K,n+1}$ vs. $Y_{K,n}$ $(K=\mathrm{A,B,C,D})$ for $\theta_C^*=-0.05334$. The points thus-generated lie along the curves which look like quadric curves (Fig. 3). These are typical curves of chaotic response.

To understand the characteristics of stability, we have computed the Liapunov exponents

$$\lambda_K=\frac{1}{N}\sum_{i=1}^{N}\ln\left|\frac{dF_K}{dY_K}\right|_i,$$

where $N=26$. The computational results are as follows: $\lambda_A=0.326$, $\lambda_B=0.333$, $\lambda_C=0.461$, and $\lambda_D=0.346$. Because λ_K are all larger than zero, the asymptotic motion form of the

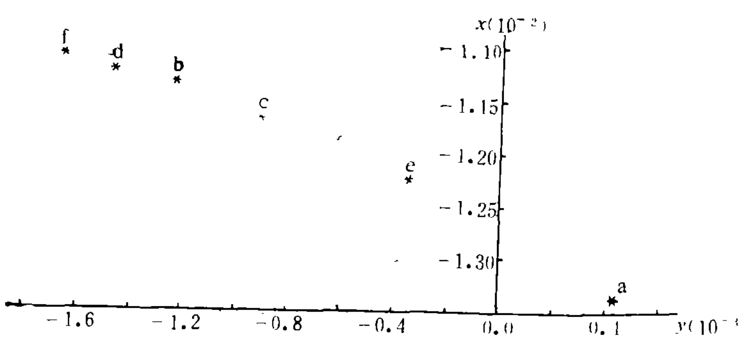

Fig. 4 Surface of section plots for $\theta_C^*=-0.053382$.

system of Eqs. (8)—(13) for $\theta_C^*=-0.05334$ corresponds to a strange attractor.

In the chaotic region with $\theta_C^*<r_\infty$, we have observed the appearance of stable three-point and six-point periodic cycles which can be called periodic windows. For example, within the limits of $-0.053384\leqslant\theta_C^*\leqslant-0.053382$ there is a stable periodic cycle with six fixed points (Fig. 4). Along with the decrease of the value of θ_C^*, apparently chaotic behavior reappears.

V. CONCLUSIONS AND DISCUSSIONS

Charney and Devore (1979) put forward the concept of multiple equilibria of the atmospheric circulation. Recently, a lot of research on multiple equilibria of both high-low index circulation and subtropical flow patterns, and on transforms among multiple equilibria has been conducted by Chinese meteorologists. The research usually relates with multiple equilibria and/or limit cycles, they both are very important motion forms of forced, dissipative, and nonlinear systems. Meantime, they are only a part of the evolutional processes of the systems. The whole aspect of the evolutional processes should include the intrinsic stochasticity of deterministic equations, i.e., chaotic or aperiodic behavior, and the transform processes between deterministic and stochastic motion forms. In this paper, we have obtained the aperiodic states of large scale atmospheric motion by using the low-order spectral model. The way leading to the chaotic behavior is the period-doubling bifurcations, immediately after the thermal forcing parameter reaches the critical point r_∞, the chaotic states appear. In the chaotic region there may also exhibit stable periodic windows with three or six fixed points.

The Lorenz system describing the small-scale convection in the atmosphere consists of three coupled ordinary differential equations containing two nonlinear terms. Lorenz attractor consists of two fragments. Each of them revolves, respectively, round the original fixed point suspended in the three-dimensional space in the shape of inward spiral. While approaching to the fixed point, one of them would suddenly and randomly jump to the outside of another one and continue its rotation. Rossler strange attractor consists of only one fragment. The system used here, which governs the dynamics of larger-scale baroclinic atmospheric motion, consists of eight ordinary differential equations having twelve nonlinear terms. In certain parametric combinations there may appear the chaotic behavior of larger-scale atmospheric motion. The system orbit corresponding to the chaotic state always pierces sequentially the surface of section at the points which lie on the four inter-linked fragments, but there are no stable fixed points on the fragments.

As mentioned above,in the range of $-0.039\geqslant\theta_C^*>-0.05285$, the system orbits approach to the simple stable limit cycle. It is characterized by the periodic oscillation of subtropical high at 250 hPa along the east-west direction with periods of two–three weeks. Along with the gradual change of the thermal parameter θ_C^* and the successive appearance of period-doubling bifurcations, the periods of oscillation of subtropical high increase, and some semiperiodic states occur. After θ_C^* reaches the critical point r_∞, the semiperiodic states have become the irregular oscillations. These motion forms look like those in the real atmosphere. As for the evolution of locations of subtropical high centre at the upper troposphere in summertime in the real atmosphere, there may appear distinct oscillation features: regular oscillations along the east-west direction with a period of two–three weeks, quasi-periodic motions, and irregular oscillations. Therefore, it would seem to us that there is probably the inherent relation between the maintenance and the transform of the different oscillation forms of larger-scale atmospheric motion and the gradual change of the heating field.

The multiple-equilibria of the atmospheric circulation are connected with the formation of persistent flow patterns. The limit cycles correspond to the periodic variation of flow patterns, such as the periodic oscillations of subtropical high in zonal direction. The transform among multiple equilibrium states may be related to some abrupt change of flow pattern existing in the atmosphere, such as the seasonal abrupt change of the atmospheric circulation. The appearance of chaotic behavior and the transform between chaotic and regular states are probably concerned in the suspension and reappearance of quasi-periodicity in the long-range weather process. These concepts of the nonlinear dynamics of the atmosphere are in favour for understanding the mechanism of real flow patterns and their evolutions.

REFERENCES

Asselin, R. (1972), Frequency filter for time integration, *Mon, Wea. Rev.*, **100**:487—490.

Charney, J.G. and Devore, J.G. (1979), Multiple flow equilibria in the atmosphere and blocking, *J. Atmos. Sci.*, **36**:1205—1216.

Charney, J.G. and Straus, D.M. (1980), Form-drag instability, multiple equilibria and propagating planetary waves in baroclinic, orographically forced, planetary wave systems, *J. Atmos. Sci.*, **37**:1157—1176.

Feigenbaum, M.J. (1978), Quantitative universality class for a class of nonlinear transformations, *J. Stat. Phys.*, **19**:25—39.

Lorenz, E.N. (1963), Deterministic nonperiodic flow, *J. Atmos. Sci.*, **20**:130—141.

Pedlosky, J. (1980), Chaotic and periodic behavior of finite amplitude baroclinic waves, *J. Atmos. Sci.*, **37**: 1177-1196.

Saltzman, B. (1962), Finite amplitude free convection as an initial value problem-1, *J Atmos. Sci.*, **37**:1157—1176.